

CHEM MED CHEM

CHEMISTRY ENABLING DRUG DISCOVERY

Accepted Article

Title: Stabilizing p-dithiobenzyl Urethane Linkers without Rate-Limiting Self-Immolation for Traceless Drug Release

Authors: Yiwu zheng, Yang Shen, Xiaoting Meng, Yaqi Wu, Yibing Zhao, and Chuanliu Wu

This manuscript has been accepted after peer review and appears as an Accepted Article online prior to editing, proofing, and formal publication of the final Version of Record (VoR). This work is currently citable by using the Digital Object Identifier (DOI) given below. The VoR will be published online in Early View as soon as possible and may be different to this Accepted Article as a result of editing. Readers should obtain the VoR from the journal website shown below when it is published to ensure accuracy of information. The authors are responsible for the content of this Accepted Article.

To be cited as: *ChemMedChem* 10.1002/cmdc.201900248

Link to VoR: <http://dx.doi.org/10.1002/cmdc.201900248>

Stabilizing *p*-dithiobenzyl Urethane Linkers without Rate-Limiting Self-Immolation for Traceless Drug Release

Yiwu Zheng, Yang Shen, Xiaoting Meng, Yaqi Wu, Yibing Zhao*, and Chuanliu Wu*[a]

[a] Y. Zheng, Y. Shen, X. Meng, Y. Wu, Prof. Y. Zhao, Prof. C. Wu

The MOE key laboratory of Spectrochemical Analysis and instrumentation, State Key Laboratory of Physical Chemistry of Solid Surfaces, Department of chemistry, College of Chemistry and Chemical Engineering, Xiamen University, 361005 (P.R. China)
E-mail: chlwu@xmu.edu.cn, ybzhao@xmu.edu.cn

Supporting information for this article is given via a link at the end of the document.

Abstract: Exploiting the redox-sensitivity of disulfide bonds is a prevalent strategy adopted in targeted prodrug designs. Compared with aliphatic disulfides, the *p*-thiobenzyl-based disulfides have rarely been used for prodrug designs due to their intrinsic instability caused by the low pK_a of aromatic thiols. Here, we examined the interplay between steric hindrance and the low- pK_a effect on the thiol-disulfide exchange reactions and uncovered a new thiol-disulfide exchange process for the self-immolation of *p*-thiobenzyl-based disulfides. We observed a central-leaving group shifting effect in the α,α -dimethyl substituted *p*-dithiobenzyl urethane linkers (DMTB-linkers), which leads to >2 orders of magnitude increase in disulfide stability, an extent that is significantly larger than that observed from the typical aliphatic disulfides. Particularly, the DMTB-linkers display not only a high stability, but also rapid self-immolation kinetics due to the low pK_a of the aromatic thiol, which can be used as a general and robust linkage between targeting reagents and cytotoxic drugs for targeted prodrug designs. The unique and promising stability characteristics of the present DMTB-linker would inspire the development of novel targeted prodrugs to achieve traceless release of drugs into cells.

Introduction

Cancer chemotherapies can usually benefit from targeted delivery of cytotoxic drugs into cancer cells. One of the most efficient ways to achieve targeted delivery relies on prodrug designs involving the conjugation of drug molecules to targeting agents through covalent linkers (e.g., the antibody-drug conjugates and small-molecule drug conjugates).^[1] The linkers are one of the most critical components in these prodrugs, which can respond to either endogenous stimuli in cells or in tumor extracellular microenvironments or external stimuli to release the drugs.^[2] Among the diverse linkers used for prodrug designs, disulfides have attracted extensive interests due to the large differences between the extra- and intra-cellular redox environments, which can selectively release the drug molecules inside the cells.^[3] However, to avoid the premature release of drugs during circulation in the body, disulfide linkers usually need to be stabilized by regulating the local steric or electronic environments on the linkers.^[4] As very few small-molecule drugs contain thiol groups, disulfide linkers with an easily tunable stability that are also easily amenable to drug-targeting agent conjugations have usually been a virtue for prodrug designs. Despite the merits of disulfide linkers, the presence of an appended thiol to the free drug has been found detrimental to

the cytotoxic activity of the anticancer drug.^[5] It has been known that reduction of cytotoxicity for drugs bearing a free thiol group may be caused by thiol-disulfide exchange reactions between the thiol-bearing drug diffusing out from the targeting cells and protein or small-molecule disulfides in the extracellular space, which leads to the formation of mixed disulfide species less capable of crossing cell membranes and killing the surrounding cells compared to the free drugs, a phenomenon that has been well-known as the “bystander effect”.^[6] Thus, to avoid the influence of extracellular thiol-disulfide exchange reactions on the “bystander effect” and to maximize cytotoxic activity of anticancer drugs, self-immolating disulfide linkers have recently been utilized for traceless drug delivery.^[5, 7]

The most prevalently used self-immolating disulfide linkers were developed on the basis of a cyclization elimination mechanism (Figure 1a).^[3a, 5] One merit of these disulfide linkers is that their stability can be easily tuned by introducing steric hindrance (i.e., methyl groups) adjacent to the disulfide bonds. The self-immolation rate and efficiency of these disulfide linkers after the cleavage is usually fast and high enough in the intracellular environments.^[8] However, we realize that the rate of self-immolation can be slow under acidic conditions such as in the endocytic or lysosomal compartments (pH 4–6) and in tumor microenvironments which have been found to be mildly acidic (pH ~6), because the thiols of these linkers usually have a pK_a of 8–9. In addition, as thiol-reducing reagents such as the glutathione (GSH) prefer attacking the less sterically hindered sulfur atoms, we also realize that the subsequent circulation of thiol-disulfide exchanges is in principle required to release the free thiol drugs ready for self-immolation, though depending on in which side of the disulfide bond the two methyl groups were introduced (Figure 1a). This disulfide shuffling circulation constitutes the rate-limiting steps for self-immolation, particularly in acidic environments where the rate of thiol-disulfide exchanges is slow.^[9] Considering that more and more prodrug designs exploit the mildly acidic tumor microenvironments and endocytic compartments as targeting locations for reduction-induced drug release,^[2b, 10] novel self-immolating disulfide linkers with both good stability and robust self-immolation capability under these specific environments are definitely a valuable module for the development of novel cytotoxic prodrugs.

An alternative route for the design of self-immolating disulfide linkers relies on the 1,6-benzyl elimination mechanism.^[11] However, these disulfide linkers have rarely been used for prodrug designs, because they are usually ~2–3 orders of magnitude less stable than the conventional aliphatic disulfides,

though disulfide linkers of this type (i.e., *p*-thiobenzyl-based disulfide) were developed over 20 years ago and their capability of self-immolation under physiological conditions is even more robust than the aforementioned self-immolating disulfides.^[11b, 11c] The intrinsic instability of the *p*-thiobenzyl-based disulfides can be elucidated by Brønsted equation, which indicates that the lower pK_a (~6) of the aromatic thiol can accelerate the cleavage of the disulfides by serving as a favorable leaving group.^[12] In general, the effect of steric hindrance on disulfide stability can be less pronounced than the electronic effect. For example, the presence of 1–2 methyl groups can usually increase stability of disulfide bonds by 5- to 20-folds in comparison to unhindered bonds.^[4b, 13] Thus, it is important to examine to what extent the *p*-thiobenzyl-based disulfides can be stabilized by manipulation of steric hindrance and if the steric hindrance can compensate for the low- pK_a induced instability to afford useful linkers for cytotoxic prodrug designs. Though there have been a few reports showing that the stability of *p*-thiobenzyl-based disulfides can indeed be increased by introducing one or two methyl groups adjacent to the disulfide bonds,^[14] it remains unclear how the interplay between steric hindrance and low- pK_a effect affects the thiol-disulfide exchange reactions, and how these reactions further react on the self-immolation of the *p*-thiobenzyl-based disulfides.

In this work, we examined the effect of the steric hindrance of two methyl groups adjacent to the *p*-thiobenzyl-based disulfides on their thiol-disulfide exchange reactions with small thiol-reducing reagents and how these reactions affect the subsequent 1,6-benzyl elimination of the *p*-thiobenzyl group. We found that the low- pK_a aromatic thiol prefers serving as the central group for nucleophilic attacking rather than as leaving group, because the aliphatic thiol is too sterically hindered to be attacked (Figure 1b). This central-leaving group shifting effect results in >2 orders of magnitude increase in stability in GSH buffers in comparison to the unhindered analogue. After the disulfide reduction, the GSH-mixed intermediate is subject to a rapid exchange reaction with another GSH molecule to further release the free thiol form of the *p*-thiobenzyl molecule ready for self-immolation (Figure 1b). Considering that the low pK_a of aromatic thiols can afford the *p*-thiobenzyl-based disulfides rapid self-immolation kinetics upon reduction even under mildly acidic conditions, targeted prodrugs were then designed and synthesized using a stabilized *p*-dithiobenzyl urethane, folic acid (FA) and Doxorubicin (DOX) or monomethyl auristatin E (MMAE) as a linker, a targeting agent and an anticancer drug, respectively. We demonstrated that the free cytotoxic drugs can be efficiently released into the cytosol by exploiting the mildly acidic and reducing endocytosis pathways mediated by folate receptor (FR) as a targeting location for the reduction cleavage and self-immolation. A FRET probe that enables us to visualize the drug release processes was also developed, which clearly demonstrates the performance of the *p*-dithiobenzyl urethane linker for endocytosis-based prodrug release. This work thus not only reveals a central-leaving group shifting effect for stabilizing *p*-thiobenzyl-based disulfide bonds, but provides useful self-immolating disulfide linkers for targeted cytotoxic prodrug designs.

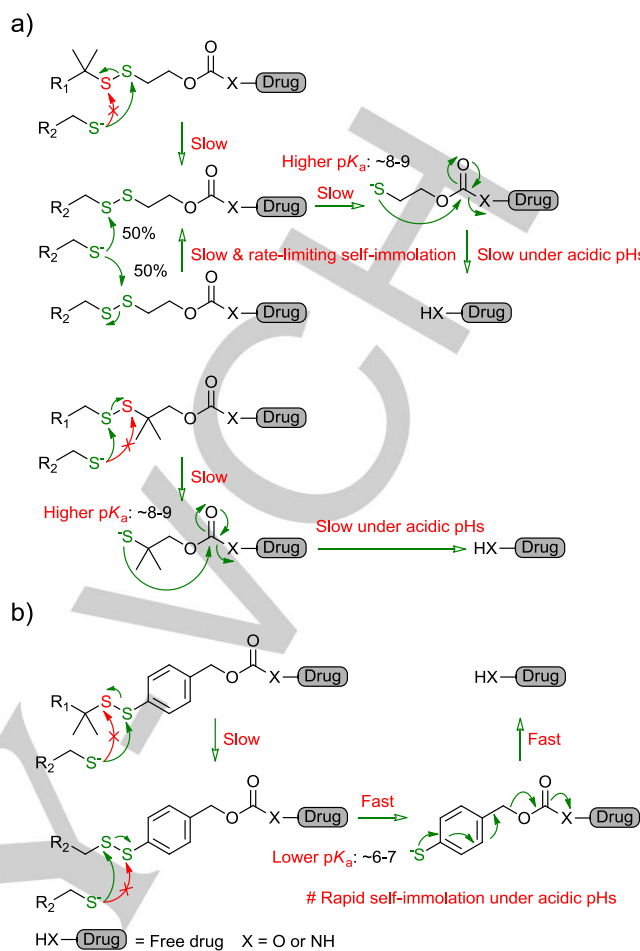


Figure 1. a) Generic thiol-disulfide exchange reactions for the cleavage of typical aliphatic disulfides and cyclization-based elimination processes. b) Thiol-disulfide exchange reactions taking place during the cleavage and self-immolation of the DMTB linkers.

Results and Discussion

To examine the effect of steric hindrance on the stability of *p*-thiobenzyl-based disulfides, a cysteine (Cys) analog, penicillamine (Pen, β,β -dimethylcysteine), which has two methyl groups adjacent to the thiol and two functional groups amenable to further modifications was chosen in our study.^[15] In addition, to facilitate the monitoring of the thiol-disulfide exchanges using high performance liquid chromatography (HPLC),^[16] short peptides with good water solubility were used as a straightforward and flexible platform for presenting the Cys and Pen thiol. Thus, Cys-containing peptide (P1), Pen-containing peptide (P2) and 4-mercaptobenzeneacetate (MBA, thiol pK_a : 5.95)^[17] were used as models to synthesize the mixed disulfides (i.e., M1: unhindered *p*-thiobenzyl-based disulfide; M2: α,α -dimethyl substituted *p*-dithiobenzyl-based disulfide) (Figure 2a). HPLC chromatograms shown in Figure 2b reveal the cleavage process of the 10 μ M M1 in 0.2 mM glutathione (GSH) at pH 7.4. We found that GSH can selectively attack the aliphatic sulfur atom, which results in the rapid formation of MBA and P1-GSH mixed disulfide and the negligible formation of P1. This result indicates that the nucleophilic attack on mixed disulfides ($R'SSR''$, $pK_a^{R'SH} > pK_a^{R''SH}$) would occur favorably with the

release of the more acidic thiol (R"SH). By contrast, when 10 μ M M2 was incubated in 0.5 mM GSH at pH 7.4, we observed a gradual decrease of M2 associated with an increase of P2 and MBA-GSH mixed disulfide, and MBA-GSH is subsequently reduced by a reaction with another GSH molecule to give the MBA (Figure 2c). It is worth mentioning that the formation of minor amount of P2-GSH mixed disulfide should be resulted from the further thiol-disulfide exchanges between P2 and GSSG. To further demonstrate that the aromatic thiol can act as

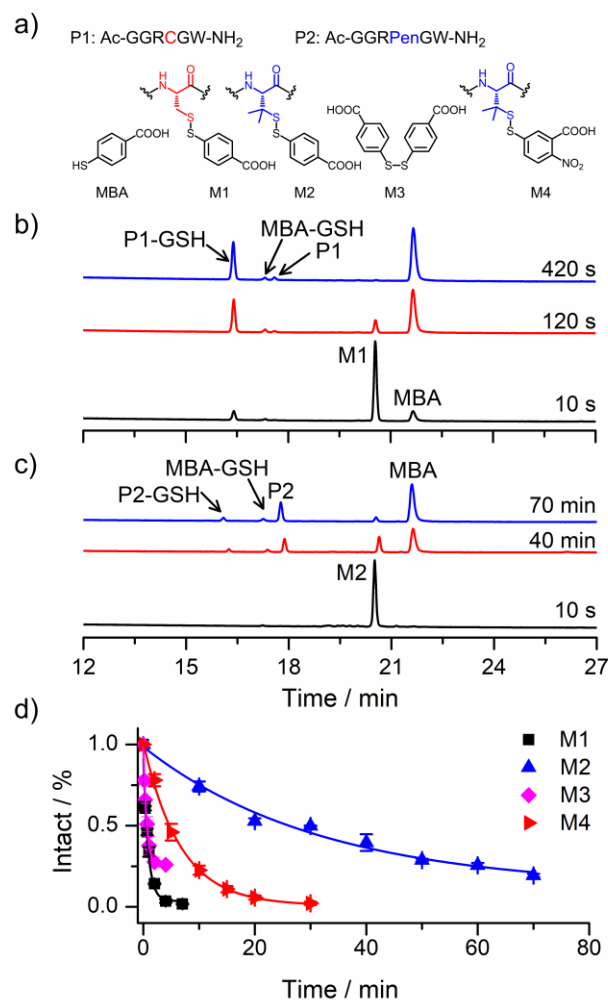


Figure 2. a) Chemical structure of disulfide linkers; note that flanking residues in peptides were omitted (P1: Ac-GGRCGW-NH₂; P2: Ac-GGRPenGW-NH₂). b) Representative chromatograms for thiol-disulfide exchanges of M1 (10 μ M) with GSH (0.2 mM) at pH 7.4 (phosphate buffer, 100 mM); absorbance was recorded at 280 nm. c) Representative chromatograms for thiol-disulfide exchanges of M2 (10 μ M) with GSH (0.5 mM) at pH 7.4 (phosphate buffer, 100 mM); absorbance was recorded at 280 nm; the chromatograph peaks were characterized by mass spectrometry (Figure S1). d) Representative plots of disappearance of disulfide linkers as a function of time.

the central atom in thiol-disulfide exchange reactions, aromatic disulfide (M3) was then synthesized, and the rate of cleavage of M3 is very rapid in 0.2 mM GSH at pH 7.4 with a half-life of 37.6 s (Figure 2d), suggesting that GSH can attack the M3 sulfur atom. In stark contrast to the aromatic disulfide, Pen-S-S-Pen disulfide is extremely stable even in 10 mM GSH buffers.^[4a]

These results show that the cleavage of the α,α -dimethyl substituted disulfides by thiol-disulfide exchanges relies on the nucleophilic attack of the MBA sulfur atom (as a central group), and the α,α -dimethyl substituted sulfur mainly serves as the leaving group due to steric hindrance.

We then examined and compared the kinetics of cleavage of M1 and M2. The half-lives ($t_{1/2}$) can be obtained from the non-linear regression of curves shown in Figure 2d using a pseudo-first-order kinetics model. The M2 disulfide (a half-life of 26.6 min was obtained in 0.5 mM GSH at pH 7.4) is \sim 127 times more stable than the M1 disulfide (a half-life of 31.3 s was obtained in 0.2 mM GSH at pH 7.4). Furthermore, it is worth mentioning that the M2 disulfide is slightly more stable than the Cys-S-S-Pen disulfides.^[15] Additionally, the stability of the α,α -dimethyl substituted disulfides could be easily adjusted by altering the pK_a value of the aromatic thiol. As shown in Figure 2d, compared to M2 disulfide, M4 (EiSH, thiol pK_a : 4.5; $t_{1/2}$ = 4.7 min) have approximately 5.6-fold faster exchange kinetics under the same condition.

Based on the above promising results, we then used the 4-mercaptobenzyl alcohol (MA) as a self-immolative unit to design α,α -dimethyl substituted p-dithiobenzyl urethane linkers (DMTB-linkers) for targeted cytotoxic prodrug designs. Folic acid (FA) is employed as a targeting ligand for the design, because it has a very high affinity to folate receptor (FR)-overexpressed cells.^[10b] FR is overexpressed in many tumors, which can actively internalize the bound folates into cells via recycling endosomal pathways.^[18] The recycling endosomal pathways have been found reducing,^[19] which can be potential locations for disulfide reduction. We designed and synthesized a DMTB-linked folate-doxorubicin (DOX) conjugates (D1) for targeted delivery of DOX to the FR-overexpressed cancer cells (Figure 3a). D1 was synthesized by coupling a thiophilic heterobifunctional cross-linker to the DOX by the activated carbonate chemistry first, followed by a substitution of the 2-thiopyridyl group of the linker with a FA-containing penicillamine (see the Supporting Information for the details). We first examined if the treatment of the D1 with GSH can result in a release of the active drug. Indeed, D1 was completely converted to DOX in the presence of 10 mM GSH within 5 h at pH 7.4 (Figure 3b). In addition, we evaluate the kinetics of cleavage of the D1 in the presence of 10 mM and 0.2 mM GSH at pH 7.4 phosphate buffer solutions, which mimics the redox environments in the cytosol and in the blood circulation, respectively. The reconversion kinetics of the DOX prodrug D1 was rapid in 10 mM GSH with a half-life of 1.3 h, but the prodrug D1 are extremely stable in 0.2 mM GSH, the percentage of cleavage is only 8% after 6 h incubation (Figure 3c), which meets the demand that FA-drug conjugates can usually be eliminated from the blood circulation with a half-life of around half of an hour.^[20] Of note, it is likely that the hydrophobic stacking interaction between the ligand and the drug as well as the negatively charged microenvironment surrounding the disulfide bond should contribute to the remarkable increase in the stability of the DMTB-linker, which is reflected by the slow kinetics of cleavage compared to the kinetics shown in Figure 2b). This result indicates that the DMTB-linker shows not only a rapid responsiveness to highly reducing conditions, but an ultrahigh stability in the weakly reducing extracellular

environments such as in the blood circulation. We next examined if the prodrug D1 would take advantage of the reducing power in the recycling endosomal for drug release. The prodrug D1 was incubated with FR-positive KB cells, D1 shows a dose-dependent inhibition of proliferation in KB cells after 48 h of incubation, as determined by Cell Counting Kit-8 (CCK-8). Free DOX was also tested in an analogous manner. The corresponding IC_{50} values were estimated to be 0.87 μ M and 3.25 μ M for the free DOX and the D1 (Table 1), respectively, indicates that the reduction of the DMTB-linker and the rapid self-immolation can take place in the mildly acidic and reducing endosomal compartment.

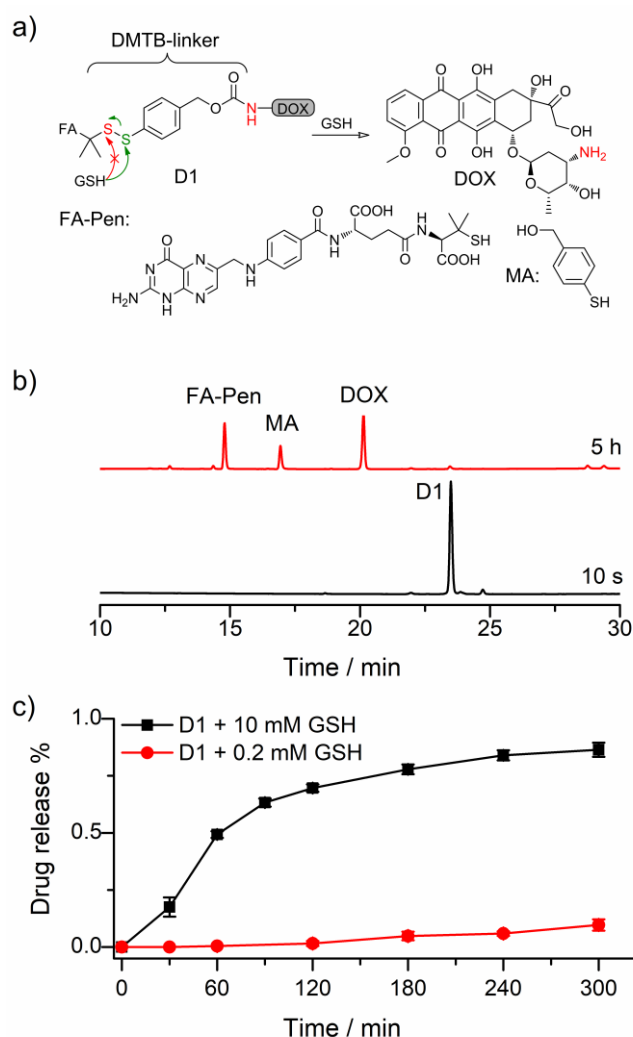


Figure 3. a) Schematic representation of the drug release process and chemical structure of FA-Pen and MA; b) HPLC chromatograms show the release of DOX from D1 (10 μ M) in the presence of 10 mM GSH at pH 7.4 after a reaction of 5 h. HPLC chromatograms were recorded at 254 nm. c) Kinetic traces for DOX release from D1 in the presence of 10 mM and 0.2 mM GSH at pH = 7.4 phosphate buffer. Data are presented as mean \pm SD ($n = 3$).

In the light of the stability characteristics of D1 in GSH buffers, we next turned our attention to the utility of the DMTB-linker for conjugating an anti-cancer drug with a higher cytotoxicity (a

microtubule inhibitor agent MMAE^[21]). The prodrug D2 was synthesized in a similar way to synthesizing D1. The release kinetics of D2 was also studied, and we obtained similar results to that from D1 (Figure 5a and Figure S2). However, D2 ($IC_{50} = 4.54$ nM) is around 1000-fold more cytotoxic than D1 (Table 1 and Figure 4), indicating the potent therapeutic effect of D2.

We then compared the DMTB-linker with the well-established self-immolating linkers based on cyclization. A prodrug C1 was synthesized for the comparison (Figure 5a), which has two methyl groups adjacent to the sulfur atom on the ligand side. Interestingly, the cytotoxic activity of D2 is slightly higher than C1 ($IC_{50} = 8.90$ nM), though the D2 disulfide has 1.5-fold slower exchange kinetics in comparison to the C1 disulfide (Figure S6) (Table 1 and Figure 4). A potential explanation for this is the complex thiol–disulfide exchange processes shown in Figure 1a. The disulfide shuffling circulation (Figure 1a) should be the rate-limiting steps for self-immolation, which slows down the release rate of free drugs. Indeed, we observed the formation of GSH-mixed MMAE (1a) when C1 was incubated in a GSH/GSSG-mixed buffer, whereas no formation of GSH-mixed MMAE (2a) was observed from D2 under the same condition (Figure 5b). Because the rate of disulfide cleavage for 2a is ~ 15 -fold faster than 1a according to the prediction of Brønsted equation,^[22] and 2a can undergo a rapid thiol–disulfide exchange reaction with GSH to directly yield 2b. In contrast, GSH can attack either of the two sulfur atoms in 1a, which results in two distinguished thiol–disulfide exchange pathways. Thus, the complete cleavage of 1a disulfide with concomitant release of 1b involves multistep thiol–disulfide exchange processes. Indeed, the formation of the unstable intermediates 2a and 2b was not observed (Figure 5b), suggesting that the kinetics of self-immolation are very fast. Overall, the promising results presented in this section indicate that the DMTB-linker provides a useful tool for developing targeted cytotoxic prodrugs.

To expand our understanding of the role that the DMTB-linked self-immolation plays in drug release and cytotoxicity, the nonself-immolative prodrug C2 with an amide conjugation was designed and synthesized (Figure 5a). The cytotoxicity of C2 to KB cells ($IC_{50} = 18.6$ nM; Table 1) was slightly lower than that of D2. In addition, MMAE-SH was also evaluated for comparison, and its IC_{50} was estimated to be 11.4 nM. The free MMAE (0.30 nM) was 38-fold more potent than MMAE-SH, indicating that the sulfhydryl modification on MMAE has a great influence on the cytotoxicity. A possible explanation is that when the disulfide is cleaved in cells to release a thiol-bearing MMAE, upon efflux out of the cells, thiol-bearing MMAE can react with disulfide-containing compounds in the extracellular space, a process that can significantly reduce the bystander effect of cytotoxic drugs.^[6b] Indeed, the thiol-bearing MMAE (MMAE-SH) is also less cytotoxicity than the S-methylated MMAE (MMAE-S-CH₃) (Table 1). In addition, we are not able to rule out the possibility that the thiol modification on the MMAE might affect its intercalation into the target tubulin proteins. To confirm the importance of the disulfide bond reduction, the non-cleavable maleimide control C3 was synthesized and evaluated; it only has very weak cytotoxicity to KB cells (Table 1 and Figure 4).

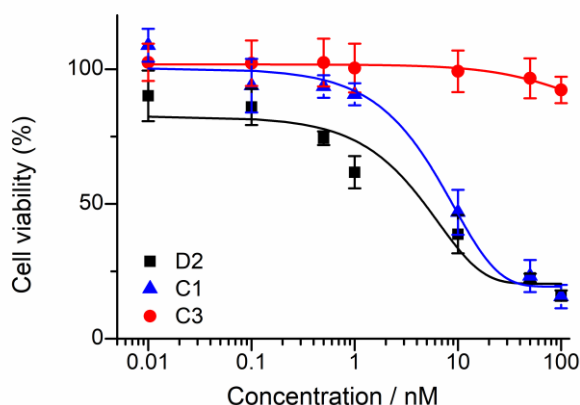


Figure 4. Dose response curves for cell viability treated with D2, C1 and C3, respectively. All compounds were incubated with the KB cells for 48 h. Data are presented as mean \pm SD ($n = 3$).

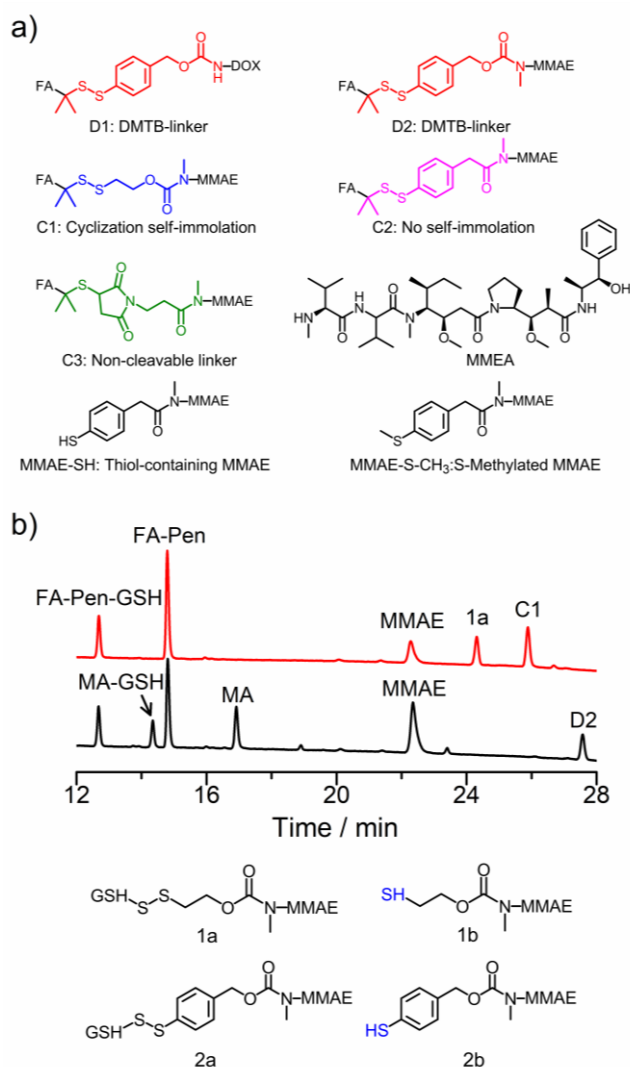


Figure 5. a) Abbreviated chemical structure of FA-Drug conjugates. b) HPLC chromatograms show the reduction of C1 and D2 (30 μ M) by GSH/GSSG (at -220 mV redox potential) in phosphate buffer pH 7.4 supplemented with 10% DMSO as co-solvent after a reaction of 3h; the peaks were characterized by mass spectrometry (Figure S7-S8). The HPLC chromatograms were recorded at 210 nm.

Table 1. *In vitro* cytotoxicity of FA-drug conjugates and free drugs to KB cells.

Compounds	Description	IC ₅₀ (nM) ^[a]
DOX	Anticancer drug	870
D1	1,6-Elimination	3250
MMAE-SH	Thiol-bearing MMAE	11.4
MMAE-S-CH ₃	S-methylated MMAE	5.14
MMAE	Anticancer drug	0.30
D2	1,6-Elimination	4.54
C1	Cyclization self-immolation	8.90
C2	No self-immolation	18.6
C3	Non-cleavable linker	>500

[a] Cell proliferation was determined after 2 days incubation using CCK-8 assays. Dose response curves for these data were presented in Figures S3-S5.

We then examined if the recycling endosomal pathways are indeed the locations where the disulfide linkers were cleaved for the release of drugs by using a DMTB-FRET probe (Figure 6). Kinetics measurements based on fluorescence were carried out in the presence of 10 mM and 0.2 mM GSH at pH 7.4 phosphate buffers. The incubation of DMTB-FRET probe in 10 mM GSH buffer led to a rapid increase of fluorescence intensity with a half-life of 0.92 h⁻¹. At 0.2 mM GSH concentration, only a negligible fluorescence recovery was observed after 6 h incubation (Figure S9). In addition, the boron dipyrromethene (BODIPY) fluorophore is very suitable for mimicking the behavior of the anticancer drugs (MMAE and DOX) in living cells due to their similar hydrophobic properties. Thus, DMTB-FRET probe can serve as a fluorescent prodrug mimic for the fluorescent monitoring of the targeted cellular uptake and the subsequent drug release process. Interestingly, intense intracellular fluorescence was observed after the incubation of cells with the DMTB-FRET probe (Figure 6b), though a portion of green fluorescence merged well with the red fluorescence (LysoTracker Red DND-99) from the lysosomes. However, the coincubation of N-(3-maleimidopropionyl)biotin (MPB, a potent blocker for cell-surface thiols and thiols in the endocytosis pathways^[23]) with the DMTB-FRET probe during the cell culture can result in a complete suppression of the DMTB-linker reduction (Figure 6c). These results indicate that the reduction of the DMTB-linker takes place on the cell surface, or during the early stages of uptake. This result suggests that the reduction of DMTB-linker stems only from thiol-disulfide exchange reactions, thus excluding other possible ways of disulfide reduction, though the detailed mechanism of disulfide reduction in reducing compartments is still unknown. To distinguish the relative contribution of the cell surface and the early stages of endocytosis to DMTB-linker reduction, KB cells were incubated with DMTB-FRET probe at 4 °C (to inhibit endocytosis); and no

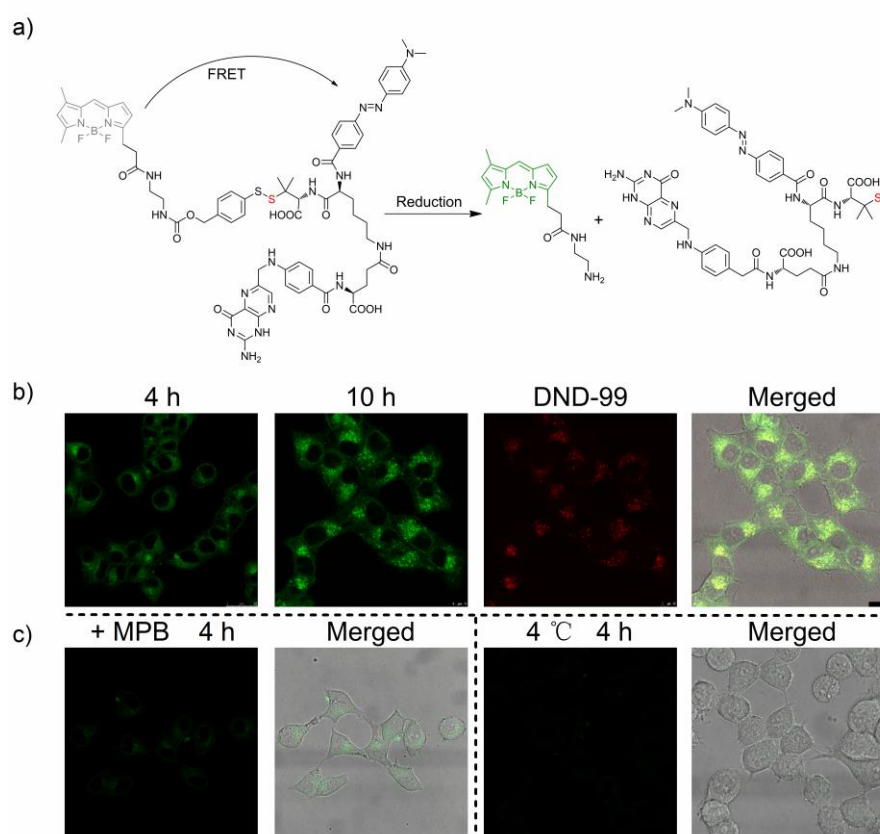


Figure 6. a) Design of DMTB-FRET probe based on intramolecular energy transfer mechanism. b) Confocal fluorescence images of KB cells incubated with the DMTB-FRET probe at 37°C, evolution of fluorescence was observed with time. LysoTracker Red DND-99 (DND-99) was used to track cell lysosomes. c) Confocal fluorescence images of KB cells treated with DMTB-FRET probe over 4h in the presence of MPB and at 4°C. Scale bar: 10 μ m.

fluorescence inside cells was observed (Figure 6c), suggesting that the cell surface was not involved in the fluorescence recovery. These results suggest that the mildly acidic reducing endosomal milieu is strongly involved in the reduction of the DMTB-FRET probe (Figure 7a).

Finally, we examined the stability of DMTB in the presence of fetal bovine serum (FBS). As can be seen in Figure 7b, the recovery of fluorescence is extremely slow in 50% FBS buffer. When 50% FBS was supplemented with 10 mM GSH, as expected, a very rapid dequenching was observed. In addition, when the probes were co-incubated in 50% serum with N-ethylmaleimide (NEM, a thiol capping reagent), no change of fluorescence intensity was observed over time, indicating that the cleavage of DMTB was resulted mainly from thiol-disulfide exchange reactions. These results demonstrate the excellent stability of the DMTB linker in serum.

Conclusions

In summary, we examined the effect of two methyl groups adjacent to the p-thiobenzyl-based disulfides on their thiol-disulfide exchange reactions and elucidated the mechanism of the p-dithiobenzyl-based disulfides reduction and self-immolation. A central-leaving group shifting effect was observed

in our DMTB-linkers, which leads to >2 orders of magnitude increase in disulfide stability, an extent that is significantly larger than that observed from the typical aliphatic disulfides. Particularly, the DMTB-linkers display not only a high stability, but also rapid self-immolation kinetics due to the low pK_a of the aromatic thiol, which can be a useful tool for developing targeted cytotoxic prodrugs. Indeed, the DMTB-linked cytotoxic prodrugs exhibit a high potency in killing cancer cells. A DMTB-FRET probe was also designed and synthesized to enable us to monitor the process of DMTB-linked prodrug release. Rapid release of cytotoxic drugs in recycling endosomal pathways mainly contribute to the high potency of the prodrugs. Recently, non-internalizing targeted prodrugs which take advantage of reduction of disulfide-linked prodrugs on the tumor cell-surface microenvironments have been found to be of high efficiency in anticancer therapy.^[24] However, considering that the reduction of conventional aliphatic disulfides in the tumor microenvironments can usually lead to unavoidable formation biothiols-linked drugs with weaker bystander killing capability,^[25] our DMTB-linked prodrug design provides an alternative strategy to solve this problem. Achieving high stability in blood circulation without comprising fast drug release is of fundamental importance to targeted prodrug design. We believe that novel targeted prodrug designs would greatly benefit from the stability characteristics of the present DMTB-linker.

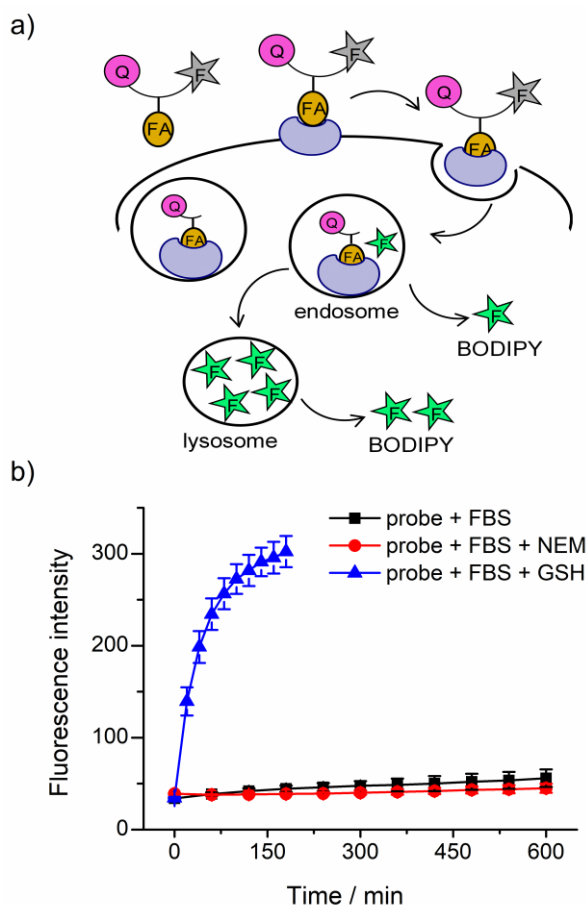


Figure 7. a) Schematic representation of the reduction of DMTB-FRET probe through the recycling endosomal route. b) Thioli-disulfide exchange kinetics of DMTB-FRET probe (0.1 μM) in 50% FBS at pH 7.4 (black line), 50% FBS at pH 7.4 pretreated with 0.2mM NEM for 2 h (red line), and 50% FBS supplemented with 10 mM GSH (blue line). Data are presented as mean \pm SD ($n = 3$).

Experimental Section

Kinetics of thiol–disulfide exchanges and drug release: All solutions used in kinetic studies were deoxygenated by bubbling with nitrogen in a round-bottomed flask sealed with a rubber stopper. To further exclude oxygen, experiments were carried out in an anaerobic incubator. In a typical experiment, 10 μM peptide disulfide or prodrugs were incubated with 0.2 or 0.5 mM reducing agent (GSH) in pH 7.4 phosphate buffers. At predefined times, disulfide exchanges were quenched by addition of an equal volume of 10% meta-phosphoric acid. The samples were then analyzed by UPLC or HPLC.

Kinetics of DMTB-FRET cleavage in redox buffers: Stock solution of DMTB-FRET probe (50 μM) was prepared in DMSO. The concentration of the probe was calculated spectrophotometrically ($\epsilon_{500\text{ nm}} = 86652\text{ cm}^{-1}\cdot\text{M}^{-1}$). In a typical experiment, FRET-DMTB probe (final concentration: 100 nM) was incubated with GSH solution (0.2 mM or 10 mM in 100 mM degassed phosphate buffer; pH 7.4). At predefined intervals, the fluorescence of the solution ($\lambda_{\text{ex}} = 488\text{ nm}$; $\lambda_{\text{em}} = 511\text{ nm}$) was measured using a fluorescence spectrometer.

Kinetics of DMTB-FRET cleavage in Serum: 150 μL of fetal bovine serum (FBS) and 147 μL phosphate buffer (100mM, pH 7.4) were added into a fluorescence cuvette. Then, 3 μL of a 50 μM stock solution of DMTB-FRET probe was added. At predefined intervals, the fluorescence

($\lambda_{\text{ex}} = 488\text{ nm}$; $\lambda_{\text{em}} = 511\text{ nm}$) was measured using a fluorescence spectrometer. To block thiol-disulfide exchanges in serum, pre-treat FBS with 0.2 mM N-ethylmaleimide (NEM) for 2 h. Then, 3 μL of a 50 μM stock solution of DMTB-FRET probe was added and fluorescence was measured with time.

Cell culture: KB cells were cultured in DMEM medium (high glucose) containing 10 % FBS and 1 % penicillin/streptomycin (penicillin: 10,000 U $\cdot\text{mL}^{-1}$, streptomycin: 10,000 U $\cdot\text{mL}^{-1}$) under an atmosphere of 5% CO_2 at 37 $^\circ\text{C}$. Cells were passaged at about 80 % cell confluency using a 0.25 % trypsin solution.

Cell viability assay: Cytotoxicity of prodrugs and MMAE-derived drugs was evaluated by Cell Counting Kit-8 (CCK-8). KB cells were seeded in a 96-well plate at an initial cell density of 8000 cells per well and grown overnight at 37 $^\circ\text{C}$, 5 % CO_2 . On the second day, the supernate was removed and 100 μL prodrugs in DMEM (without FBS) was added to each well at several different concentrations, the cells were incubated at 37 $^\circ\text{C}$, 5 % CO_2 for 48 h. Then the cell viability was measured using CCK-8 according to the manufacturer's protocol. The absorbance was then measured at 450 nm using an ELIASA reader (PerkinElmer Enspire). The obtained absorbance was blank-corrected (blank: DMEM+CCK-8, no cells) and the cell viability in percent was calculated according to the following equation:

$$\text{Cell viability} = (\text{OD}_{450, \text{sample}} / \text{OD}_{450, \text{control}}) \times 100\%$$

where $\text{OD}_{450, \text{sample}}$ represents the optical density of the cells treated with prodrugs and $\text{OD}_{450, \text{control}}$ is the cells treated with DMEM (without FBS). Experiments were conducted in triplicate with $n = 3$. Error bars represent standard deviation of the mean.

Confocal cell imaging: KB cells were plated into glass bottom cell culture dishes at an initial cell density of 100,000 cells per well. After 24 h at 37 $^\circ\text{C}$, 5 % CO_2 , the cells were grown to about 80 % confluence. The medium was then removed and the cells were washed twice with PBS. Cells were then incubated with 1 mL serum-free complete medium containing 200 nM DMTB-FRET (stock solution: 50 μM in DMSO) at 37 $^\circ\text{C}$, 5 % CO_2 for desired lengths of time. For cell lysosome staining, cells were incubated with 200 nM LysoTracker Red DND-99 for 2 h. After that, cells were imaged in a Leica TCS SP5X Confocal Microscope System at different detection channels. (BODIPY channel: $\lambda_{\text{ex}} = 488\text{ nm}$, $\lambda_{\text{em}} = 510\text{-}560\text{ nm}$; LysoTracker Red DND-99 channel: $\lambda_{\text{ex}} = 543\text{ nm}$, $\lambda_{\text{em}} = 600\text{-}670\text{ nm}$).

Confocal cell imaging with MPB coinubation: Cells were seeded as described above. Upon medium removal, the cells were washed twice with PBS, coinubated with 1 mL complete medium containing 500 μM MPB (stock solution: 100 mM in DMSO) and 200 nM FRET-DMTB for 4 h. After that, cells were imaged in a Leica TCS SP5X Confocal Microscope System.

Acknowledgements

We would like to acknowledge the financial support from the National Natural Science Foundation of China (21822404 and 21675132), The fundamental Research Funds for Central Universities (20720180034), the Program for Changjiang Scholars and Innovative Research Team in University (13036), and the Foundation for Innovative Research Groups of the National Natural Science Foundation of China (21521004).

Keywords: Disulfide • Traceless drug release • Self-immolating linkers • Penicillamine • *p*-Dithiobenzyl urethane

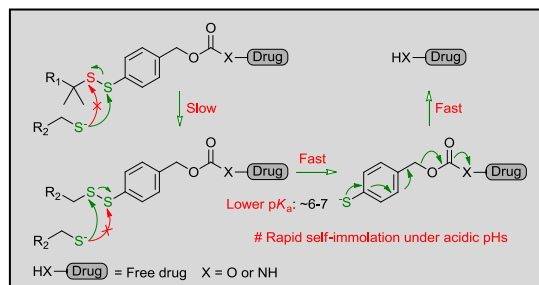
References:

- [1] G. Casi, D. Neri, *J. Med. Chem.* **2015**, *58*, 8751-8761.

- [2] a) L. R. Staben, S. G. Koenig, S. M. Lehar, R. Vandlen, D. Zhang, J. Chuh, S. F. Yu, C. Ng, J. Guo, Y. Liu, A. Fourie-O'Donohue, M. Go, X. Linghu, N. L. Segraves, T. Wang, J. Chen, B. Wei, G. D. Phillips, K. Xu, K. R. Kozak, S. Mariathasan, J. A. Flygare, T. H. Pillow, *Nat. Chem.* **2016**, *8*, 1112-1119; b) G. J. Bernardes, G. Casi, S. Trussel, I. Hartmann, K. Schwager, J. Scheuermann, D. Neri, *Angew. Chem. Int. Ed.* **2012**, *51*, 941-944; c) Y. Zheng, J. Ren, Y. Wu, X. Meng, Y. Zhao, C. Wu, *Bioconjugate Chem.* **2017**, *28*, 2620-2626; d) R. M. Versteegen, R. Rossin, W. ten Hoeve, H. M. Janssen, M. S. Robillard, *Angew. Chem. Int. Ed.* **2013**, *52*, 14112-14116.
- [3] a) M. H. Lee, J. L. Sessler, J. S. Kim, *Acc. Chem. Res.* **2015**, *48*, 2935-2946; b) L. Brulisauer, M. A. Gauthier, J. C. Leroux, *J. Control. Release* **2014**, *195*, 147-154.
- [4] a) C. Wu, S. Wang, L. Brulisauer, J. C. Leroux, M. A. Gauthier, *Biomacromolecules* **2013**, *14*, 2383-2388; b) B. A. Kellogg, L. Garrett, Y. Kovtun, K. C. Lai, B. Leece, M. Miller, G. Payne, R. Steeves, K. R. Whiteman, W. Widdison, H. Xie, R. Singh, R. V. Chari, J. M. Lambert, R. J. Lutz, *Bioconjugate Chem.* **2011**, *22*, 717-727.
- [5] D. Zhang, T. H. Pillow, Y. Ma, J. d. Cruz-Chuh, K. R. Kozak, J. D. Sadowsky, G. D. Lewis Phillips, J. Guo, M. Darwish, P. Fan, J. Chen, C. He, T. Wang, H. Yao, Z. Xu, J. Chen, J. Wai, Z. Pei, C. E. C. A. Hop, S. C. Khojasteh, P. S. Dragovich, *ACS Med. Chem. Lett.* **2016**, *7*, 988-993.
- [6] a) W. C. Widdison, J. F. Ponte, J. A. Coccia, L. Lanieri, Y. Setiady, L. Dong, A. Skaletskaya, E. E. Hong, R. Wu, Q. Qiu, R. Singh, P. Salomon, N. Fishkin, L. Harris, E. K. Maloney, Y. Kovtun, K. Veale, S. D. Wilhelm, C. A. Audette, J. A. Costoplus, R. V. Chari, *Bioconjugate Chem.* **2015**, *26*, 2261-2278; b) X. Sun, W. Widdison, M. Mayo, S. Wilhelm, B. Leece, R. Chari, R. Singh, H. Erickson, *Bioconjugate Chem.* **2011**, *22*, 728-735.
- [7] a) J. D. Sadowsky, T. H. Pillow, J. Chen, F. Fan, C. He, Y. Wang, G. Yan, H. Yao, Z. Xu, S. Martin, D. Zhang, P. Chu, J. Dela Cruz-Chuh, A. O'Donohue, G. Li, G. Del Rosario, J. He, L. Liu, C. Ng, D. Su, G. D. Lewis Phillips, K. R. Kozak, S. F. Yu, K. Xu, D. Leipold, J. Wai, *Bioconjugate Chem.* **2017**, *28*, 2086-2098; b) S. Maiti, N. Park, J. H. Han, H. M. Jeon, J. H. Lee, S. Bhuniya, C. Kang, J. S. Kim, *J. Am. Chem. Soc.* **2013**, *135*, 4567-4572; c) Z. Pei, C. Chen, J. Chen, J. D. Cruz-Chuh, R. Delarosa, Y. Deng, A. Fourie-O'Donohue, I. Figueroa, J. Guo, W. Jin, S. C. Khojasteh, K. R. Kozak, B. Latifi, J. Lee, G. Li, E. Lin, L. Liu, J. Lu, S. Martin, C. Ng, T. Nguyen, R. Ohri, G. Lewis Phillips, T. H. Pillow, R. K. Rowntree, N. J. Stagg, D. Stokoe, S. Ulufatu, V. A. Verma, J. Wai, J. Wang, K. Xu, Z. Xu, H. Yao, S. F. Yu, D. Zhang, P. S. Dragovich, *Mol. Pharm.* **2018**, *15*, 3979-3996.
- [8] T. H. Pillow, J. D. Sadowsky, D. Zhang, S. F. Yu, G. Del Rosario, K. Xu, J. He, S. Bhakta, R. Ohri, K. R. Kozak, E. Ha, J. R. Junutula, J. A. Flygare, *Chem. Sci.* **2017**, *8*, 366-370.
- [9] C. D. Austin, X. Wen, L. Gazzard, C. Nelson, R. H. Scheller, S. J. Scales, *Proc. Natl. Acad. Sci. U. S. A.* **2005**, *102*, 17987-17992.
- [10] a) N. Joubert, C. Denevault-Sabourin, F. Bryden, M. C. Viaud-Massuard, *Eur. J. Med. Chem.* **2017**, *142*, 393-415; b) I. R. Vlahov, C. P. Leamon, *Bioconjugate Chem.* **2012**, *23*, 1357-1369.
- [11] a) L. H. Qian, J. Q. Fu, P. Y. Yuan, S. B. Du, W. Huang, L. Li, S. Q. Yao, *Angew. Chem. Int. Ed.* **2018**, *57*, 1532-1536; b) T. Sun, A. Morger, B. Castagner, J. C. Leroux, *Chem. Commun.* **2015**, *51*, 5721-5724; c) P. D. Senter, W. E. Pearce, R. S. Greenfield, *J. Org. Chem.* **1990**, *55*, 2975-2978.
- [12] R. Freter, E. R. Pohl, J. M. Wilson, D. J. Hupe, *J. Org. Chem.* **1979**, *44*, 1771-1774.
- [13] E. K. Lei, S. O. Kelley, *J. Am. Chem. Soc.* **2017**, *139*, 9455-9458.
- [14] L. Greenfield, W. Bloch, M. Moreland, W. B. Lawrence Greenfield, and Margaret Moreland, *Bioconjugate Chem.* **1990**, *1*, 400-410.
- [15] Y. Zheng, L. Zhai, Y. Zhao, C. Wu, *J. Am. Chem. Soc.* **2015**, *137*, 15094-15097.
- [16] C. Wu, C. Belenda, J. C. Leroux, M. A. Gauthier, *Chem. Eur. J.* **2011**, *17*, 10064-10070.
- [17] J. D. Gough, W. J. Lees, *J. Biotechnol.* **2005**, *115*, 279-290.
- [18] S. Sabharanjak, S. Mayor, *Adv. Drug. Deliv. Rev.* **2004**, *56*, 1099-1109.
- [19] J. Yang, H. Chen, I. R. Vlahov, J. X. Cheng, P. S. Low, *Proc. Natl. Acad. Sci. U. S. A.* **2006**, *103*, 13872-13877.
- [20] J. Li, E. A. Sausville, P. J. Klein, D. Morgenstern, C. P. Leamon, R. A. Messmann, P. LoRusso, *J. Clin. Pharmacol.* **2009**, *49*, 1467-1476.
- [21] A. Maderna, C. A. Leverett, *Mol. Pharm.* **2015**, *12*, 1798-1812.
- [22] J. D. Gough, R. H. Williams, A. F. Donofrio, W. J. Lees, *J. Am. Chem. Soc.* **2002**, *124*, 3885-3892.
- [23] L. Brulisauer, G. Valentino, S. Morinaga, K. Cam, J. Thostrup Bukrinski, M. A. Gauthier, J. C. Leroux, *Angew. Chem. Int. Ed.* **2014**, *53*, 8392-8396.
- [24] G. Casi, D. Neri, *Mol. Pharm.* **2015**, *12*, 1880-1884.
- [25] E. Perrino, M. Steiner, N. Krall, G. J. Bernardes, F. Pretto, G. Casi, D. Neri, *Cancer Res.* **2014**, *74*, 2569-2578.

Entry for the Table of Contents

Insert graphic for Table of Contents here. ((Please ensure your graphic is in **one** of following formats))



Insert text for Table of Contents here.

We examined the effect of two methyl groups adjacent to the *p*-thiobenzyl-based disulfides on their thiol-disulfide exchange reactions and elucidated the mechanism of the *p*-dithiobenzyl-based disulfides reduction and self-immolation. We observed a central-leaving group shifting effect in these *p*-thiobenzyl-based disulfide linkers, which leads to >2 orders of magnitude increase in disulfide stability. This work thus not only reveals a central-leaving group shifting effect for stabilizing *p*-thiobenzyl-based disulfide bonds, but provides useful self-immolating disulfide linkers for targeted cytotoxic prodrug designs.

((The Table of Contents text should give readers a short preview of the main theme of the research and results included in the paper to attract their attention into reading the paper in full. The Table of Contents text **should be different from the abstract** and should be no more than 450 characters including spaces.))